



Cite this: *Chem. Commun.*, 2024, 60, 1731

Received 3rd November 2023,
Accepted 11th January 2024

DOI: 10.1039/d3cc05433k

rsc.li/chemcomm

Bridge improvement work: maximising non-linear optical performance in polyoxometalate derivatives†

Claire F. Jones,^a Bethany R. Hood,^a Yovan de Coene,^b Ivan Lopez-Poves,^a Benoît Champagne,^b Koen Clays^b and John Fielden^a

New phenyl and stilbene-bridged polyoxometalate (POM) charge-transfer chromophores with diphenylamino donor groups produce, respectively, the highest intrinsic and absolute quadratic hyperpolarisabilities measured for such species. The $\beta_{0,zzz}$ obtained for the phenyl bridge – at 180×10^{-30} esu – is remarkable for a short conjugated system while changing to the stilbene (260×10^{-30} esu) produces a substantial increase in non-linearity for a minimal red-shift in the absorption profile. Together with TD-DFT calculations, the results show that maximising conjugation in the π -bridge is vital to high performance in such “POMophores”.

Polyoxometalates (POMs) are a diverse class of anionic molecular metal oxide clusters, which encompass a diverse range of properties.¹ This range of properties can be expanded, and tuned through formation of hybrid POM-organic materials – for example by ion-pairing,² more specific supramolecular interactions,³ and by covalent derivatisation.⁴ Due to enforced spatial proximity and (in some cases) through-bond electronic communication, covalent derivatisation gives the greatest potential for significantly adjusting the intrinsic properties of the POM such as redox potentials,^{4b} and for emergence of physical properties not found independently in either subunit, for example long-range photo-induced charge separation.⁵

The strongest POM-organic electronic communication is seen in arylimido derivatives, where direct conjugation of the POM core

and aromatic system occurs through the metal-nitrogen multiple bond, resulting in new electronic transitions and strongly shifted redox potentials.^{4e,6} We have exploited this unmatched electronic communication to construct molecular charge-transfer chromophores (POMophores) based on arylimido-Lindqvist ($[\text{Mo}_6\text{O}_{18}\text{NAr}]^{2-}$) acceptor units attached to a number of organic donor groups and π -bridges.⁷ These materials have shown high 2nd order non-linear optical (NLO) coefficients, β , particularly considering their relatively high visible transparency and small π -systems. They can also have significant 3rd order properties,⁸ and recently demonstrated reversible, redox switched NLO responses.⁹ Thus, such POMophores have the potential to yield high-activity, switchable NLO materials while avoiding problems for efficiency and stability that result from reabsorption of second harmonic (SH) light.

However, there is still much to learn about basic structure-property relationships in POMophores. To date our work has predominantly featured dimethylamino donor groups, with phenyl or phenylacetylene bridges, yet a diphenylamino ($-\text{NPh}_2$) donor gave the highest static hyperpolarizability (β_0).^{7c} Herein, we expand the family of $-\text{NPh}_2$ donor POMophores showing a consistent performance advantage for $-\text{NPh}_2$ over $-\text{NMe}_2$, and suggested by prior calculations,¹⁰ introduce an alkene bridge for the first time obtaining the highest β_0 yet for a POMophore.

Compounds **1** to **3** (Fig. 1 and 2 previously published^{7c}) were obtained by synthesising the aniline precursor, then reacting with $[\text{NBu}_4]_2[\text{Mo}_6\text{O}_{19}]$ using established coupling methods (Scheme S1, ESI†).^{4e,6b,7} Synthesis of **3** by Heck coupling on an iodo-substituted POM precursor was also investigated, an

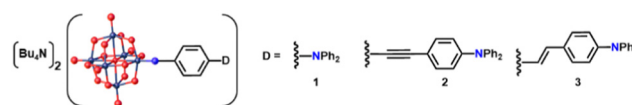


Fig. 1 POMophores **1** to **3**. Mo atoms are dark grey, O red and the imido-N blue. Compound **2** was previously published.^{7c}

^a School of Chemistry, University of East Anglia, Norwich, NR4 7TJ, UK

^b Department of Chemistry, University of Leuven, Celestijnenlaan 200D, Leuven B-3001, Belgium

^c Unit of Theoretical and Structural Physical Chemistry, Namur Institute of Structured Matter, University of Namur, Namur B-5000, Belgium

^d Department of Chemistry, Lancaster University, Lancaster, LA1 4YB, UK.

E-mail: J.Fielden@Lancaster.ac.uk

† Electronic supplementary information (ESI) available: Synthetic and other experimental/computational details, CIF file. CCDC 2305545. For ESI and crystallographic data in CIF or other electronic format see DOI: <https://doi.org/10.1039/d3cc05433k>.



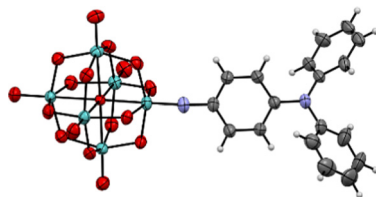


Fig. 2 X-ray crystal structure of the molecular anion in compound **1**. Disordered parts omitted for clarity, thermal ellipsoids are at the 30% probability level, C atoms are grey; Mo, green; O, red; N, blue. H atoms are white spheres of arbitrary radii. The crystal structure of **2** was previously published (CCDC 1837405†).^{7c}

approach with little precedent,¹¹ but isolation of significant quantities of the aniline derivative as well as **3** indicated that the imido bond poorly tolerates Heck conditions.

The three compounds have been characterised by multiple techniques, including X-ray crystal structures for **1** (Fig. 2, Fig. S1 and Tables S1–S3, ESI†) and **2** (previously published).^{7c} UV-vis spectra (Table 1; Fig. S2, ESI†) reveal a remarkable trend in λ_{max} for the low energy intra-hybrid charge transfer (IHCT) bands of the three POMophores: a substantial blue shift of 20 nm (0.13 eV) from phenyl bridged **1** to diphenylacetylene bridged **2**. In organic CT chromophores, including the $-\text{NO}_2$ acceptor analogues of **1** to **3**, extending conjugation invariably lowers CT transition energies,¹² while in $-\text{NMe}_2$ donor POMophores CT transitions are only very slightly higher in energy for the longer diphenylacetylene bridge.^{7b} The strong blue shift for **2** vs. **1** thus indicates a very strong influence for the donor group and bridge on the extent of charge transfer to the POM – whereby in **1** more involvement of the POM effectively lengthens the conjugation pathway and lowers the HOMO–LUMO energy gap. In compound **3**, stronger planar conjugation resulting from the alkene rather than alkyne bridge restores the transition to slightly lower energy than in **1**.

For all three compounds, TD-DFT calculations ($\omega\text{B97X-D}/6\text{-311G(d)}/\text{LanL2TZ}$, MeCN solvation by IEFPCM) reproduce experimental trends in the transition energies, and computed oscillator strengths closely follow the experimental trend in ϵ (Table 1 and Fig. S2 and S4, ESI†). Blue shifts of *ca.* 0.3 eV vs. experiment reflect the fact that these vertical excitation energies do not account for geometry relaxation of the excited state, or vibronic structure.¹³ The computed NTOs confirm that charge transfer is from the organic group to the POM, and qualitatively show greater participation of the POM in the acceptor (particle)

Table 1 UV-vis absorption data for the low energy IHCT band, and electrochemical data for **1** to **3** in acetonitrile

$\lambda_{\text{max}}/\text{nm}$ (ϵ , $10^3 \text{ M}^{-1} \text{ cm}^{-1}$) ^a	E_{max}/eV ^a	HWHM/ nm	E_{max} (calcd)/ eV ^b (f)	$E_{1/2}$ vs. $\text{Fe}^{0/+}$ / $V(\Delta E/\text{mV})$ ^c
1 434 (34.3)	2.86	33	3.22 (1.18)	−1.003 (76)
2 414 (45.3)	2.99	46	3.30 (2.43)	−0.949 (80)
3 437 (43.5)	2.84	46	3.17 (2.40)	−0.964 (72)

^a Concentrations *ca.* 10^{-5} M in MeCN. ^b TD-DFT computed value ($\omega\text{B97X-D}/6\text{-311G(d)}/\text{LanL2TZ}$). ^c Solutions *ca.* 10^{-3} M in analyte, 0.1 M in $[\text{NBu}_4][\text{BF}_4]$ at a glassy carbon working electrode, scan rate 100 mV s^{-1} . Ferrocene internal reference, $\Delta E_p = 74 \text{ mV}$.

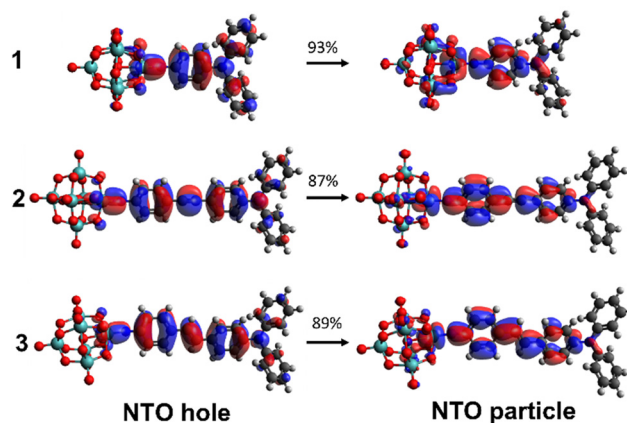


Fig. 3 TD-DFT calculated ($\omega\text{B97X-D}/6\text{-311G(d)}/\text{LanL2TZ}$) NTOs for the dominant transitions of the IHCT bands of **1** to **3**. MeCN solvation is provided by IEFPCM.

orbitals for **1** than for **2** or **3** (Fig. 3). This is reflected in computed ground-to-excited state dipole moment changes ($\Delta\mu$, Table S4, ESI†) that are almost identical in **1** to **2** and **3**, and a charge transfer distance (d_{CT} , Table S4, ESI†) only 20% shorter for **1**, despite its much shorter conjugated bridge. Natural population analysis (NPA) of the ground states (Fig. S5, ESI†) is also consistent with more effective donor–acceptor communication in **1**, through a higher calculated NPA negative charge on the $\{\text{Mo}_6\text{O}_{18}\}$ unit and a less negative NPA charge on the $-\text{NPh}_2$ donor than in either **2** or **3**.

Electrochemical measurements (Table 1 and Fig. S3, ESI†) show $[\text{Mo}_6\text{O}_{18}\text{NR}]^{2-/3-}$ reductions for all three compounds that are highly reversible on the CV timescale, however, with no steric bulk around the imido group the reduced states are not stable enough for investigation of switched properties.^{9,14} The reduction potentials $E_{1/2}$ trend more negative, in line with the trend in calculated NPA charges (Fig. S5, ESI†), as the strength of communication between $-\text{NPh}_2$ donor and POM acceptor increases across the bridge from diphenylacetylene **2**, to stilbene **3** and phenyl **1**. The negative shift for **1**, at *ca.* 55 mV vs. **2**, is rather smaller than reported for the analogous $-\text{NMe}_2$ compound,^{7b} as the availability of the N lone pair is reduced by the phenyl groups. The consequence of this is also seen in the X-ray crystal structure of **1**, where contraction of *ortho*-to-*meta*-C–C bond distances (mean 1.381(7) Å) vs. *meta*-to-*para* (mean 1.396(8) Å) is much less significant than for $-\text{NMe}_2$ (Table S3, ESI†), indicating a weaker contribution from quinoidal resonance forms.

Hyper-Rayleigh scattering (HRS) determined and TD-DFT computed β values for **1** to **3** are shown in Table 2, and a number of relevant comparisons with POM and $-\text{NO}_2$ acceptors are presented in the ESI† (Table S5, ESI†). For **2** and **3**, use of a 1064 nm fundamental gave good results, but for **1** a high level of two-photon fluorescence at 1064 nm necessitated use of a 1200 nm source. Subsequently 1200 nm was used to obtain data for all three compounds under the same conditions, and to extract non-resonant, static hyperpolarizabilities $\beta_{0,\text{zzz}}$. The results show that all three compounds have high optical



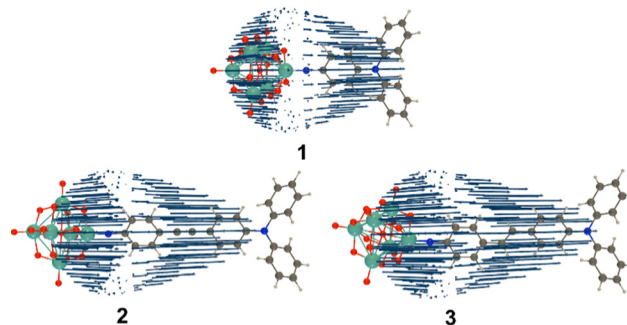
Table 2 Experimental and computed values of hyperpolarizability, β , for **1** to **3** in MeCN

	$\beta_{zzz,1064}^a$	$\beta_{zzz,1200}^a$	$\beta_{0,zzz}^b$	$\beta_{zzz,1064}$ (calcd) ^c	$\beta_{zzz,1200}$ (calcd) ^c	$\beta_0/N^{3/2d}$
	/ 10^{-30} esu					
1	—	430 \pm 30	180 \pm 10	261 (287)	199 (213)	12.2
2	590 \pm 20	376 \pm 30	174 \pm 10	373 (340)	286 (267)	3.32
3	1040 \pm 20	640 \pm 30	260 \pm 10	454 (435)	335 (328)	4.96

^a β_{zzz} calculated assuming a single dominant tensor component, measured using 1064 or 1200 nm fundamental laser beams. The quoted units (esu) can be converted into SI units ($C^3 m^3 J^{-2}$) by dividing by a factor of 2.693×10^{20} . ^b Non-resonant, static β estimated from $\beta_{zzz,1200}$ using the two state model.¹⁵ ^c TD-DFT computed value (ω B97X-D/6-311G(d)/LanL2TZ) following B-convention for comparison with experiment. Values in parentheses account for differences of frequency dispersion between experiment and calculations. ^d N = Number of electrons in π -bridge:¹⁶ 6 for **1** and 14 for **2** and **3**.

non-linearities: $\beta_{0,zzz}$ values are several times higher than reported for the technologically exploited DAS⁺ cation under non-resonant conditions and they are the three highest performing POMophores to date. The $\beta_{0,zzz}$ of **1**, at 180×10^{-30} esu, is remarkably high for such a short π -bridge – as underlined by normalisation of β_0 to N , the effective number of polarisable π -electrons in the bridge, to yield an extremely high intrinsic β ($\beta_0/N^{3/2}$), of 12.2. This more than doubles the highest intrinsic β previously obtained for a POMophore (the $-NMe_2$ analogue of **1**),^{7c} while producing only a 10 nm red-shift in λ_{max} and consequently pushing the performance well beyond the empirical $\beta_0/N^{3/2}$ vs. λ_{max} limits described by Kuzyk for planar organic chromophores.¹⁶ Similar percentage increases in smaller β values are seen in purely organic chromophores with short (*i.e.* phenyl) conjugated bridges on changing $-NMe_2/-NET_2$ for $-NPh_2/NTol_2$ donor groups, and have been ascribed to extension of donor orbitals onto the aryl groups.¹² Extending with the alkyne bridge in **2** slightly lowers β_0 , consistent with the blue shifted electronic transitions, while extending with an alkene to form **3** produces a *ca.* 50% increase in β_0 (to 260×10^{-30} esu) vs. either of the other two compounds. This is with only a 3 nm red shift in λ_{max} vs. the phenyl bridge, and while the broader IHCT band and higher ϵ of **3** results in more absorption > 450 nm, at the 600 nm SH wavelength it is quite minimal. Thus, while **1** has the highest intrinsic β of any POMophore to date, compound **3** gives the best absolute performance and retains an excellent transparency/non-linearity trade-off.

TD-DFT computed unit sphere representations (Fig. 4) indicate that the β responses are dominated by a single tensor component directed along the molecular charge transfer axis, justifying the extraction of a single β_{zzz} tensor from experiment. Dynamic β values, however, are underestimated vs experiment. In trend, they reproduce the relationship between phenyl-bridged **1** and stilbene **3** quite well, but over-estimate the non-linearity for **2** so that it is higher, rather than similar or lower than that of **1**. This is likely to reflect the fact that β values are computed for an optimised, flat geometry where the dihedral angles (ϕ) between phenyl rings and alkene or alkyne bridge are close to 0° , lacking the effects of structural fluctuations.¹⁷ Yet, while the phenyl rings of **3** have a small rotational energy barrier of only *ca.* 5 kJ mol⁻¹ between

**Fig. 4** Unit sphere representations (USRs) of the β tensor ($\lambda = 1200$ nm) of compounds **1** to **3** calculated at the IEFPCM (solvent = acetonitrile) TDDFT/ ω B97X-D/6-311G(d)/LanL2TZ level of theory. (USR factor of 0.0001).

0 and $\pm 30^\circ$, and a locally flat PES like that of trans-stilbene,¹⁸ there are substantial barriers to further rotation. For diphenylacetylenes such as **2** there is free rotation at room temperature with an energy barrier of only 2.5 kJ mol⁻¹ across all values of ϕ .¹⁹ This means that less well conjugated rotamers contribute much more to the experimental measurements on **2** and lower β . Inspection of the computed NTOs (Fig. 2) shows that in **1**, the donor orbitals extend strongly onto the $-NPh_2$ rings: compared to $-NMe_2$, this will result in a larger $\Delta\mu$ explaining the large (100%) increase in β (Table S5, ESI[†]). As the chromophores are extended, NTO holes extend less onto the $-NPh_2$ rings and NTO particles extend less onto the POMs, so that $\Delta\mu$ and d_{CT} only increase minimally with apparent conjugation length. A corresponding trend is seen in plots of computed ground-to-excited state electron density change (Fig. S6, ESI[†]). This reduces the performance advantage for the POM/ $-NPh_2$ combination compared to other POM-based and organic chromophores. Nonetheless, the $\beta_{0,zzz}$ for **3** is *ca.* 30% higher than its nitro analogue (202×10^{-30} esu, Table S5, ESI[†]) on the same set up, showing that the increased conjugation provided by the alkene-bridge enables the POM acceptor to clearly exceed the performance of $-NO_2$ in an extended structure for the first time.

In summary, we have synthesised two new NLO-active POMophores with phenyl and stilbene bridges and diphenylamino donor groups, producing the highest intrinsic and absolute β_0 values yet reported for such compounds. Together with the previously published diphenylacetylene-bridge analogue, these results show that a key for maximising the performance advantages of the imido-Lindqvist acceptor is to maximise the strength of conjugation across the organic bridge. Work to test other, stronger donor groups, and extended planar π -bridges, is under way.

In addition to the ESI[†] and deposited cif files, data can be obtained by contacting the corresponding author, and will be deposited at DOI: <https://doi.org/10.17635/lanaster/researchdata/649>.

We thank the EPSRC for support through grant EP/M00452X/1 to J. F., X-ray data were obtained in facilities established by EPSRC grant EP/S005854/1. BRH thanks the University of East Anglia for a studentship and Lancaster University for short-term postdoctoral support. C. F. J. and



J. F. acknowledge funding from the Leverhulme Trust (RPG-2020-365) and thank Dr Joseph Wright of the University of East Anglia for assistance in re-synthesis of **3**. YDC acknowledges the Fonds Wetenschappelijk Onderzoek (FWO) for junior postdoc (No. 1234222N). Calculations were performed on the UEA High Performance Cluster, Consortium des Equipements de Calcul Intensif (CECI, <https://www.ceci-hpc.be>) and the Technological Platform of High-Performance Computing, for which the authors acknowledge the financial support of the FNRS-FRFC, the Walloon Region, and University of Namur (Conventions No. 2.5020.11, U.G006.15, U.G018.19, U.G011.22, 1610468, and RW/GEQ2016).

Conflicts of interest

There are no conflicts to declare.

Notes and references

- (a) C. L. Hill, *Chem. Rev.*, 1998, **98**, 1; (b) M. Hutin, M. H. Rosnes, D. L. Long and L. Cronin, *Comprehensive Inorg. Chem. II*, 2nd edn, 2013, vol. 2, pp. 241.
- (a) P. Bolle, C. Menet, M. Puget, H. Serier-Brault, S. Katao, V. Guerschais, F. Boucher, T. Kawai, J. Boixel and R. Dessapt, *J. Mater. Chem. C*, 2021, **9**, 13072; (b) Y. Gao, M. Choudhari, G. K. Such and C. Ritchie, *Chem. Sci.*, 2022, **13**, 2510.
- (a) M. Han, J. Hey, W. Kawamura, D. Stalke, M. Shionoya and G. H. Clever, *Inorg. Chem.*, 2012, **51**, 9574; (b) Y. Wu, R. Shi, Y.-L. Wu, J. M. Holcroft, Z. Liu, M. Frascioni, M. R. Wasielewski, H. Li and J. F. Stoddart, *J. Am. Chem. Soc.*, 2015, **137**, 4111; (c) C. Falaise, M. A. Moussawi, S. Floquet, P. A. Abramov, M. N. Sokolov, M. Haouas and E. Cadot, *J. Am. Chem. Soc.*, 2018, **140**, 11198; (d) B. Zhang, W. Guan, F. Yin, J. Wang, B. Li and L. Wu, *Dalton Trans.*, 2018, **47**, 1388.
- (a) A. V. Anyushin, A. Kondinski and T. N. Parac-Vogt, *Chem. Soc. Rev.*, 2020, **49**, 382; (b) A. J. Kibler, N. Tsang, M. Winslow, S. P. Argent, H. W. Lam, D. Robinson and G. N. Newton, *Inorg. Chem.*, 2023, **62**, 3585; (c) A. Dolbecq, E. Dumas, C. R. Mayer and P. Mialane, *Chem. Rev.*, 2010, **110**, 6009; (d) A. Proust, B. Matt, R. Villanneau, G. Guillemot, P. Gouzerh and G. Izzet, *Chem. Soc. Rev.*, 2012, **41**, 7605; (e) J. Zhang, F. Xiao, J. Hao and Y. Wei, *Dalton Trans.*, 2012, **41**, 3599.
- (a) F. Odobel, M. Séverac, Y. Pellegrin, E. Blart, C. Fosse, C. Cannizzo, C. R. Meyer, K. J. Elliott and A. Harriman, *Chem. – Eur. J.*, 2009, **15**, 3130; (b) K. J. Elliott, A. Harriman, L. Le Pleux, Y. Pellegrin, E. Blart, C. R. Mayer and F. Odobel, *Phys. Chem. Chem. Phys.*, 2009, **11**, 8767; (c) B. Matt, X. Xiang, A. L. Kaledin, N. Han, J. Moussa, H. Amouri, S. Alves, C. L. Hill, T. Lian, D. G. Musaev, G. Izzet and A. Proust, *Chem. Sci.*, 2013, **4**, 1737; (d) B. Matt, J. Fize, J. Moussa, H. Amouri, A. Pereira, V. Artero, G. Izzet and A. Proust, *Energy Environ. Sci.*, 2013, **6**, 1504.
- (a) J. B. Strong, G. P. A. Yap, R. Ostrander, L. M. Liable-Sands, A. L. Rheingold, R. Thouvenot, P. Gouzerh and E. A. Maatta, *J. Am. Chem. Soc.*, 2000, **122**, 639; (b) Y. Wei, B. Xu, C. L. Barnes and Z. Peng, *J. Am. Chem. Soc.*, 2001, **123**, 4083.
- (a) A. Al-Yasari, N. Van Steerteghem, H. El Moll, K. Clays and J. Fielden, *Dalton Trans.*, 2016, **45**, 2818; (b) A. Al-Yasari, N. Van Steerteghem, H. Kearns, H. El Moll, K. Faulds, J. A. Wright, B. S. Bruntschwig, K. Clays and J. Fielden, *Inorg. Chem.*, 2017, **17**, 10181; (c) A. Al-Yasari, P. Spence, H. El Moll, N. Van Steerteghem, P. N. Horton, B. S. Bruntschwig, K. Clays and J. Fielden, *Dalton Trans.*, 2018, **47**, 10415.
- A. Al-Yasari, H. El Moll, R. Purdy, K. B. Vincent, P. Spence, J.-P. Malval and J. Fielden, *Phys. Chem. Chem. Phys.*, 2021, **23**, 11807.
- B. R. Hood, Y. de Coene, A. V. Torre Do Vale Froes, C. F. Jones, P. Beaujean, V. Liégeois, F. MacMillan, B. Champagne, K. Clays and J. Fielden, *Angew. Chem., Int. Ed.*, 2023, **62**, e202215537.
- E. Rtibi and B. Champagne, *Symmetry*, 2021, **13**, 1636.
- Y. Zhu, L. Wang, J. Hao, P. Yin, J. Zhang, Q. Li, L. Zhu and Y. Wei, *Chem. – Eur. J.*, 2009, **15**, 3076.
- (a) C. R. Moylan, R. J. Twest, V. Y. Lee, S. A. Swanson, K. M. Betterton and R. D. Miller, *J. Am. Chem. Soc.*, 1993, **115**, 12599; (b) C. M. Whitaker, E. V. Patterson, K. L. Kott and R. J. McMahon, *J. Am. Chem. Soc.*, 1996, **118**, 9966.
- F. Zutterman, V. Liégeois and B. Champagne, *ChemPhotoChem*, 2017, **1**, 281.
- B. R. Hood, PhD thesis, University of East Anglia, 2022.
- (a) J. L. Oudar and D. S. Chemla, *J. Chem. Phys.*, 1977, **66**, 2664; (b) J. L. Oudar, *J. Chem. Phys.*, 1977, **67**, 446.
- (a) K. Tripathy, J. Pérez Moreno, M. G. Kuzyk, B. J. Coe, K. Clays and A. M. Kelley, *J. Chem. Phys.*, 2004, **121**, 7932; (b) K. Clays and B. J. Coe, *Chem. Mater.*, 2003, **15**, 642.
- F. Castet, C. Tonnelé, L. Muccioli and B. Champagne, *Acc. Chem. Res.*, 2022, **55**, 3716.
- M. M. Lin, D. Shorokhov and A. H. Zewail, *J. Phys. Chem. A*, 2009, **113**, 4075.
- (a) M. Wierzbicka, I. Bylí, C. Czaplowski and W. Wiczak, *RSC Adv.*, 2015, **5**, 29294; (b) K. Okuyama, T. Hasegawa, M. Ito and N. Mikami, *J. Phys. Chem.*, 1984, **88**, 1711.

